Diffusion in Lipid Monolayers Studied by Fluorescence Correlation Spectroscopy

Alina Joukainen Nielsen

January 6, 2006

Bachelor Project
Membrane Biophysics Group
Niels Bohr Institute
University of Copenhagen
Supervisor: Thomas Heimburg

Abstract

The physics of lipid membranes is a hot topic at the moment, because the hitherto accepted model of the biological membraneof a cell, Singer and Nicolson's 'fluid mosaic' model, seems to need a serious amount of revision. In the fluid mosaic model, the only function of the lipids is to provide a barrier between the cell's cytoplasm and the surroundings and an anchor for the membrane proteins [22]. However, new scientific investigations suggest, that the lipid molecules play other important roles, when it comes to cell function. Therefore, the general physical properties of lipids are thoroughly investigated at the moment, and this thesis is an attempt to play along.

The aim of this thesis is to measure the diffusion of lipid molecules in simple model membranes, as a function of surface pressure. Monolayers of one kind of lipid were used, and the means by which diffusion was measured, was the technique of Fluorescence Correlation Spectroscpy (FCS). FCS has never been used on monolayers before, so the results are brand new.

The diffusion constants are found to decrease with increasing surface pressure, in the pressure range of existence of the monolayer.

Isotherms of the lipid used have been measured in order to find the interesting values of the pressure, for which to measure diffusion constants.

Furthermore, Fluorescence Microscopy images have been recorded to visually see the domain formation of lipids in different phases, at conditions of coexistence.

Resume

Lipidmembraners fysik er et varmt emne for tiden, da den hidtil accepterede model for den biologiske cellemembran, Singer og Nicolson's 'fluid mosaic' model ser ud til at have brug for en kraftig revision. I denne model, er lipidernes funktioner udelukkende at virke som en barriere mellem cellens cytoplasma og dens omgivelser, og som anker for membranproteinerne [22]. Nye videnskabelige undersøgelser tyder imidlertid på, at lipidmolekylerne spiller andre vigtige roller, hvad angår cellens funktion. Derfor undersøges lipiders generelle fysiske egenskaber nu flittigt, og dette projekt er et forsøg på at deltage i den opgave.

Målet med dette projekt er at måle lipidmolekylers diffusion i simple modelmembraner, som en funktion af overfladetryk. Monolag af en enkelt type lipid blev benyttet, og diffusionen blev målt ved hjælp af metoden 'Fluorescence Correlation Spectroscopy' (FCS)- fluorescens korrelationsspektroskopi. Denne metode er aldrig blevet anvendt på monolag før, så de observerede resultater er helt nye.

Diffusionskonstanterne findes at aftage ved øget overfladetryk i det trykinterval, som monolaget eksisterer i.

Der er målt isotermer af den type lipid, der er blevet anvendt i FCS-forsøgene for at finde ud af, hvilke værdier af trykket, der var interessante at måle diffusionskonstanter ved.

Herudover er der blevet optaget fluorescens-mikroskopibilleder, for visuelt at se, hvordan lipider i forskellige faser danner domæner ved koeksistens.

Alina Joukainen Nielsen
cpr.nr. 300380-1178

Contents

Chapter 1

Introduction

1.1 Biological Membranes

Every living cell is surrounded by a membrane, as are all of its organelles[1] (Fig.1.1). These membranes consist of a variety of molecules, the most abundant of these being the lipids. In biological membranes the lipids form a so-called bilayer (Fig.1.2).

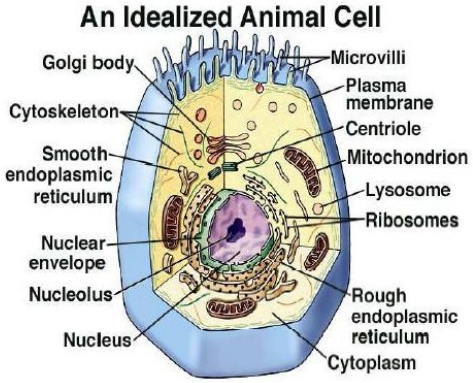

Figure 1.1: An animal cell with a variety of different organelles [2].

This bilayer acts as a barrier between the cell's cytoplasm and its environment, and likewise encloses the organelles. Real biological membranes are extremely complex, containing many different types of lipids, and also proteins embedded in the bilayer.

1.2 Lipids and domain formation

A lipid molecule consists of a polar, hydrophilic (literally 'water-loving') head group and usually two hydrophobic (literally 'water-hating') fatty acid chains. All experiments in this thesis have been done with the lipid DMPC (DiMyristoyl Phosphatidyl-Choline) (Fig.1.3). In aqueous environments, lipids form aggregates, so that the heads

[1] Organelles are structures inside the cell that have important functions, e.g. the nucleus, mitochondria and the Golgi apparatus.

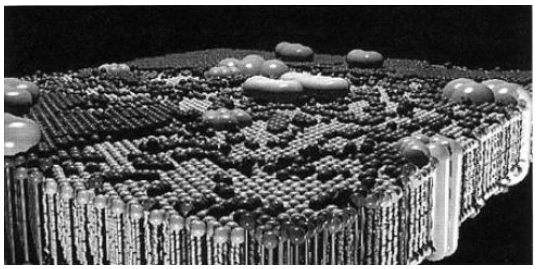

Figure 1.2: Lipid bilayer with inserted proteins (large molecules) [1], by courtesy of H. Seeger (NBI).

are in contact with the water, and the tails are not. Lipids are able to form several different types of structures that satisfy their amphiphilic desires (Fig.1.4), one of these being the mentioned bilayer. However, this thesis focuses on a structure called the lipid monolayer, which I will descibe in section 1.3. For now I will just mention, that the one-lipid monolayer will do as a simple model for a biological membrane.

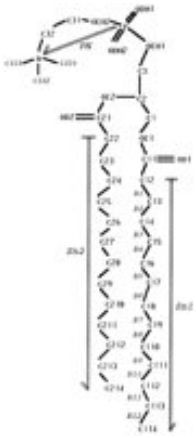

Figure 1.3: DMPC molecule [15].

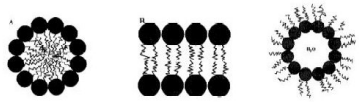

Figure 1.4: Examples of membrane structures: micelle, bilayer and inverse hexagonal phase [2].

Lipid structures can exist in different phases, depending on temperature, pressure, etc. The two most important phases in the physiological temperature regime are the so-called 'solid ordered', or 'gel' phase, and the so-called 'liquid disordered', or 'fluid' phase. In the gel phase, the lipid chains are highly ordered, and the lipid head groups are arranged in a 2-dimensional lattice. In the fluid phase, the chains are disordered, and the head groups are randomly distributed in the plane of the membrane. A phase transition takes place, from the gel to the fluid phase, if we for instance raise the temperature of the system across the melting temperature of the membrane (Fig.1.5). Naturally, there are conditions under which the two phases can coexist.

In the case of coexistence, the gel and fluid lipids are not distributed randomly across the membrane. Instead, they form domains of solid and liquid molecules (Fig.1.2). This is probably due to the different effective lengths of the lipid chains in the two

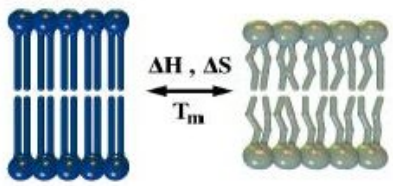

Figure 1.5: Melting transition in a lipid bilayer [2].

phases (Fig.1.5). Domain formation seems to be the best way to isolate the hydrophobic chains from the surrounding aqueous environment. Interestingly, it seems that biological membranes are always in a state of coexistence between the two mentioned phases [1].

Due to the complex composition of a biological membrane, natural domains will contain a mixture of chemically different kinds of lipids. How the different kinds of lipids arrange themselves in differently composite domains, depends on the chemical characteristics of the lipids, as well as on several properties of the entire system (temperature, pressure, etc.).

Special types of domains have recently been discovered and are of great interest to scientists. These are the so-called 'lipid rafts', and the lipids in these domains are mainly cholesterol and sphingolipids.

As explained in [1], many important processes in biological membranes are composed of cascades of biochemical reactions between different proteins. If these proteins have chemically different affinities for different domains of the membranes (if they are easier dissolved in some domains than in others), then they are not allowed to interact, and the processes of which they are responsible are hindered. However, the domain arrangements can be altered by enzymes, changes in pH or temperature, etc., and if it is altered in a way, that allows the proteins to interact, then the processes concerned take place. In this way, the lipids might control quite a lot of the function of cells and organelles.

1.3 Lipid Monolayers

Lipid monolayers are membranes, that consist, as the name suggests, of a single layer of lipids. Upon contact with water, they can only exist on the surface. The polar heads are then in direct contact with the water, while the tails stick out in the open air (Fig.1.6). In studying diffusion processes, the main advantage of using lipid monolay-

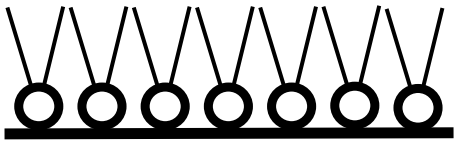

Figure 1.6: Coarse schematic diagram of a monolayer. The head groups and chains of the lipids are shown, but the arrangement of the chains is not to be taken seriously.

ers is, that we are able to control the lateral pressure. This can be easily varied by the use of two barriers that let the water diffuse freely under them, but control how much area is available to the surface molecules. Details on this method will follow in section 3.1.

Furthermore, we need only worry about lateral diffusion of the lipids. Diffusion between different layers of lipids, known as transverse diffusion or flip-flop, is excluded.[2] It is also much easier to work with monolayers than, for instance, vesicles of bilayers (unilamellar vesicles), since we can work with very large monolayers. In the experiments performed for this thesis, the monolayers are about $20 - 200\ cm^2$ in area (and about $2.5\ nm$ thick), whereas unilamellar vesicles, which are also popular experimental objects, are often made with a diameter of $100\ nm$. If something unexpected happens in an experiment involving a monolayer, one can often see what has gone wrong, with the naked eye (dust particles can for instance be seen, as they make the surface uneven). Vesicles, though, are much too small for this.

Monolayers show many of the same interesting properties, that bilayers do. For instance, they form domains on coexistence between the gel and fluid phases. This does not seem as logical as in the case of bilayers, since the hydrophobic lipid chains are protected from the water surface in a monolayer, no matter how the lipids arrange themselves, as long as the hydrophilic head groups are in contact with the water. However, the lipids seem to prefer arrangements that protect the chains from the surrounding environment, even when this environment is air. This could very likely be due to humidity of the air, although it is beyond the scope of this thesis to find out. In section 4.3 I will show some nice images of DMPC domains in monolayers.

According to [3], the first definite historical reference to the technique of spreading fatty molecules on water surfaces is made by Aristotle. In a translation by Hett (1937), he states, that 'Oil poured on to water makes it more transparent'. Pliny the Elder (Gaius Plinius Secundus AD 77) later states, in a translation by Rackham (1964), that 'again everybody is aware that ... all sea water is made smooth by oil, and so divers sprinke oil from their mouth because it calms the rough element and carries light down with them ... .' Benjamin Franklin carried out (now famous) experiments on the Clapham ponds in 1774, through which he confirmed the calming influence of oil on water surfaces, even when the layer of oil could only be a few nanometres thick. About a decay later, Agnes Pockels created monolayers of stearic acid in her own home, and found the thickness of the monolayer to be $2.3\ nm$. A value very close to the modern value for the length of the stearic acid molecule, which is $2.5\ nm$. This shows, that the molecules in her monolayers must have been closely packed and standing erect on the water surface. It was Rayleigh who proposed, a few years later (1899), that Pockels layers were, in fact, monolayers, and that they therefore gave a measure of molecular dimensions. In 1917 Langmuir carried out systematic studies of monolayers of several amphiphilic molecules, and he was the first to formulate a general theory of adsorbed films. For this and other great contributions to chemistry, physics and engineering, he recieved the Nobel Prize in Chemistry in 1932 [11], and the technique of creating monolayers now bears his name; the Langmuir technique.

Development of novel techniques and enhancement of traditional techniques have

[2] It should be noted, that transverse diffusion is usually much slower than lateral diffusion, but it is nevertheless nice to avoid the extra complexity.

over the last couple of decays made a huge contribution to the study of Langmuir monolayers. Synchrotron x-ray-diffraction experiments, monolayer-sensitive microscopy techniques, such as fluorescence microscopy, polarized fluorescence microscopy and Brewster-angle microscopy have all contributed significantly to the understanding of this type of lipid aggregate. See [4] for a brief, but more detailed summary of the most important Langmuir monolayer literature.

1.4 Diffusion

Diffusion can be understood as the independent *Brownian motion* of the molecules that make up the system. Brownian motion[3] is caused by the random collisions of the molecules with each other, which cause each one to undergo a so-called *random walk*. As mentioned in section 1.3, only lateral diffusion needs to be considered in monolayers. More on diffusion will follow in 2.2. During the experiments for this thesis, I have measured diffusion velocities in DMPC monolayers by the following method.

1.5 Method

In order to measure the diffusion under changing pressure, the author has developed a new method together with Martin Gudmand of the Membrane Biophysics Group at the Niels Bohr Institute of Copenhagen. This method is a combination of the Langmuir technique of creating lipid monolayers, and *Fluorescence Correlation Spectroscopy*, or *FCS*. FCS is a method of measuring diffusion velocities; by marking a sample of the molecules of interest with proper fluorescent molecules (also called fluorophores) and illuminating the sample with a laser, one can measure the photons emitted by the excited fluorophores, when in the laser focus, and determine, through a statistical process known as correlation, how much time the marked molecules, on average, spend in this focus. The focus, which has a Gaussian cross section, has to be so small, that each molecule contributes substantially to the measured signal, i.e. only a few molecules are simultaneously detected. As will be shown in section 2.3, one can determine the average velocity of the molecules, once the average time spent in the focus is known.

In 1974, Magde, Elson and Webb published a paper, that described the first experimental application of FCS [13]. FCS has since become an established experimental procedure and is used to measure diffusion constants[4], rate constants for chemical reactions, excited-state molecular dynamics etc.

In 1984, Möhwald and Lösche constructed the first setup to combine Fluorescence and Langmuir monolayers [12]. They performed Fluorescence Microscopy (not FCS) on DPPC (DiPalmitoyl PhosphatidylCholine) and DMPA (DiMyristoyl Phosphatic Acid) monolayers.

The new and interesting feature of our setup is the fact, that we use FCS on lipid monolayers, and thereby measure diffusion constants of the lipids as a function of lat-

[3] Named after the english botanist Robert Brown, who studied pollen grains with a microscope in 1827 [16].

[4] A diffusion constant is a measure of the diffusion velocity.

eral pressure. Pressure variation of lipid diffusion constants has never been measured before (or at least never been published).

The technical details of the Langmuir technique and FCS will be described in further detail in sections 3.1 and 3.2.

Nice images of DMPC domains have been created using Fluorescence Microscopy. It is exciting to actually see the solid domains floating in the elsewhere liquid membrane. The technical details of this procedure will follow in section 3.3.

The experimental goal of this thesis is an attempt to measure diffusion constants of lipids in a monolayer as a function of lateral pressure. This has never been done before.

If this attempt yields good results, important general information on the physics of lipid membranes may have been derived. Also, if the new method is successfully tested, it can be used in the future for more elaborate experimental investigations of lipids.

Chapter 2

Theory

2.1 Langmuir monolayers

As mentioned in the introduction, a great advantage of using lipid monolayers in the laboratory is, that one is able to control the lateral pressure in the membrane,[1] and it is possible to measure the pressure as a function of the mean molecular area, or MMA. Different lipids will show different profiles of a plot of this kind (Fig.2.1)

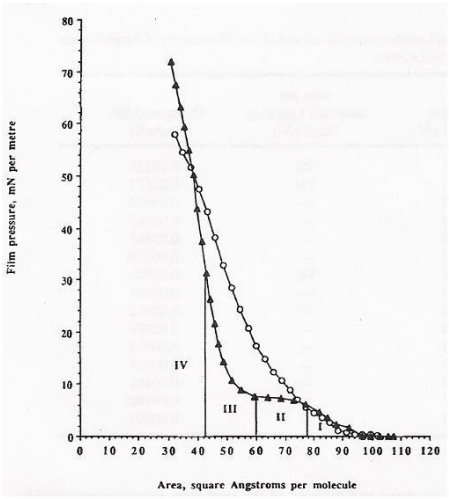

Figure 2.1: Isotherms of DMPC and DPPC, another lipid, both plotted at 21 °C. DMPC points are circles, and DPPC points, black triangles [23].

It is customary to call the plots of pressure versus MMA isotherms, and I will adopt this usage in the following. We see clearly on the isotherms, the pressures and MMA's at which something interesting happens. This is very useful in experiments, like the ones done for this thesis, in which one wishes to determine other physical properties of the system as a function of the pressure.

At large areas, the surface pressure of the system is set to zero (Fig.2.1). On compressing the monolayer, the molecules will on average come closer and closer

[1] The ways of doing this will be described in the next section.

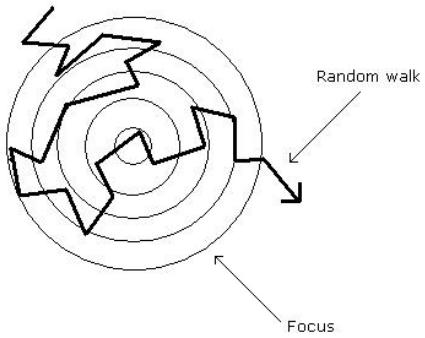

Figure 2.2: A random walk of a particle through the laser focus.

together, until finally they come in close contact. At this point, the surface pressure naturally rises. From here, the profiles can be quite different from each other.

The distinct plateau for DPPC in (Fig.2.1) indicates a phase transition with high co-operatvity, that is, high tension in the interface between ordered and disordered lipids makes it energetically very favourable for the lipids to form domains [20]. Therefore, for DPPC at $21\,^{\circ}\mathrm{C}$, there will be large domains. For DMPC, on the other hand, there is no obvious plateau in the isotherm at this temperature, and correspondingly the domains formed are very small. As is shown in section 4.3, the domains are not visible in a $150 \times 150\ \mu m$ microscopy image of the situation.

Every lipid monolayer collapses at a certain pressure. We see the collapses clearly on the measured isotherms as an almost complete lack of trend (this is not shown in Fig.2.1, but it can be seen on the measured isotherms in section 4.1). At this point in an isotherm, the pressure forces some of the lipids out of the plane of the monolayer, and as we compress further, the lipids respond by forming new structures in more layers. The surface pressure therefore does not rise as steeply anymore.

2.2 Diffusion

In the introduction, it was mentioned, that diffusion is caused by the independent Brownian motion of the particles that make up the system. Fig.2.2 shows an example of a random walk through the laser focus. This thesis investigates only lateral, translational diffusion. In this case, the motion of a single molecule is described by the Einstein-Smoluchowski relation [2]:

$$\langle r(t)^2 \rangle = 4D_\tau t \tag{2.1}$$

where $\langle r(t)^2 \rangle = \langle |r(t+\tau) - r(t)|^2 \rangle$ is the *mean square displacement* of the molecule, i.e. the average of the square of the distance travelled during time t. D_τ is the so-called *diffusion constant*. It is this parameter, that has been measured in the FCS experiments for this thesis. It can be seen from 2.1, that D_τ is a positive quantity, and that a high diffusion constant implies high diffusion speed (a high D_τ means a long distance travelled by the molecule during time t) and likewise, that a low diffusion

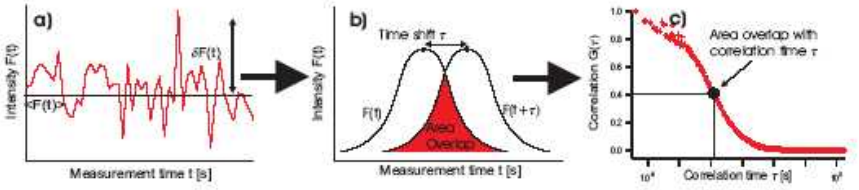

Figure 2.3: The principle of correlation, from intensity signal to correlation curve [5].

constant implies a low diffusion speed. As will be shown in section 4.2.2, for lipid systems, D_τ depends on pressure and type of lipid aggregate.

Two important consequences of Brownian motion are expressed by Fick's famous diffusion laws:

Fick's first law:

$$\vec{J} = -D_\tau \vec{\nabla} C \tag{2.2}$$

Fick's second law:

$$\frac{\partial C}{\partial t} = D_\tau \nabla^2 C \tag{2.3}$$

$\vec{J}$ is the particle flux, i.e. the number of particles that pass a given point x per second per cm^2 of area normal to the direction of diffusion (these units are those conventionally used). $\vec{\nabla} C$ is the concentration gradient,[2] and $\nabla^2 C$ is the Laplacian operator of C.[3]

These laws describe how particles in a system move from places of high concentration to places of lower concentration. The physical systems presented in this thesis contain no obvious concentration gradients, but due to small local concentration fluctuations, Fick's second law, Eq.2.3 will still be of good use in section 2.3.

2.3 Correlation

As mentioned in the introduction, FSC is about measuring the intensity of the fluorescent light emitted by labeled molecules, in order to get a measure of the average time that independent molecules spend in the laser focus. In order to find this average time, the fluorescent signal must be statistically investigated by the means of *correlation*.

Because of the small size of the focus, there will be considerable fluctuations in the fluorescent signal. At a given time, one or several fluorescent molecules may be in the laser focus, and there will also be an amount of background noise. By treating these fluctuations statistically, one is able to draw some general conclusions on the motion of the fluorescing molecules.

A typical intensity diagram is shown in Fig.2.3a. The ground level of the intensity is determined by the level of background fluorescence. The peaks arise when

[2] $\vec{\nabla} = \left(\frac{\partial}{\partial x}, \frac{\partial}{\partial y}, \frac{\partial}{\partial z}\right)$

[3] $\nabla^2 = \left(\frac{\partial^2}{\partial x^2} + \frac{\partial^2}{\partial y^2} + \frac{\partial^2}{\partial z^2}\right)$

molecules pass through the focus. The sizes of the peaks depend on the concentration of molecules and their trajectory through the focus. The intensity can be written:

$$F(t) = \langle F(t) \rangle + \delta F(t) \tag{2.4}$$

where $\langle F(t) \rangle$ is the average intensity over time, and $\delta F(t)$ the fluctuation of the intensity at time t.

Correlation is a measure of the self-similarity of the fluorescent signal after a time interval τ, the so-called *correlation time*. A high correlation means, that the intensity of the signal has not changed very much over the specified time interval, and a low correlation, that the signal is completely different. The *correlation function* contains this information [17]:

$$G(\tau) \equiv \frac{\langle \delta F(t) \cdot \delta F(t+\tau) \rangle}{\langle F(t) \rangle^2} \tag{2.5}$$

Fig.2.3b shows how the correlation works. $G(\tau)$ is proportional to the overlapping area of the two intensity functions $F(t)$ and $F(t+\tau)$. The larger the area, the greater the self-similarity of F after the time interval τ. Fig.2.3c shows a typical correlation curve, (that has in this case been normalized).

The correlation function at $\tau = 0$ gives the average number $\langle N \rangle$ of fluorescent particles in the detection volume, since the relative mean square amplitude of fluctuations of independent random molecular processes in a system is equal to the reciprocal of $\langle N \rangle$ [17]:

$$G(0) \equiv \frac{\langle [\delta F(t)]^2 \rangle}{\langle F(t) \rangle^2} = \frac{1}{\langle N \rangle} \tag{2.6}$$

This means, that when we have measured a correlation function for a sample, we can, by taking the reciprocal of the height of $G(\tau)$ at zero, determine how many molecules are on average in the focus.

As Fig.2.3c shows, we typically see a high correlation for low correlation times and zero correlation for high correlation times. This makes sense; at very low correlation times, the molecules in the laser focus have not moved very much, and the signal recorded before and after the correlation time has passed is therefore approximately the same, and for high correlation times, the situation has had time to change a lot. The mean correlation time τ_D, for which $G(\tau)$ has half its maximum value is the average time, a fluorescent molecule spends in the laser focus [5]. A high τ_D therefore indicates slow diffusion, and a low τ_D, fast diffusion.

In order to arrive at a version of the correlation function, from which one can extract the necessary information, here is a quick derivation of an analytical form of it.

The measured fluorescence intensity $F(t)$ is assumed to be proportional to the following physical quantities [2]:

q**,** the detection quantum efficiency

σ_{abs}**,** the excitation cross section of the fluorescent molecules

ϕ_f**,** the fluorescence quantum yield

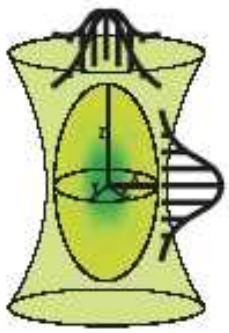

Figure 2.4: The gaussian detection volume [5].

$CEF(\vec{r})$, the collection efficiency function, i.e. the fraction of fluorescence, emitted at $\vec{r}$, that passes through the pinhole (the pinhole is presented in section 3.2) and thereby through to the detectors

$I(\vec{r})$, the excitation intensity at $\vec{r}$

$C(\vec{r},t)$, the concentration of fluorescent particles at position $\vec{r}$ at time t

$F(t)$ can thus be written

$$F(t) = q \cdot Q \cdot \int_V CEF(\vec{r}) \cdot I(\vec{r}) \cdot C(\vec{r},t) dr^3 \tag{2.7}$$

Or, writing $I_{em}(\vec{r}) = CEF(\vec{r}) \cdot I(\vec{r})$,

$$F(t) = q \cdot Q \cdot \int_V I_{em}(\vec{r}) \cdot C(\vec{r},t) dr^3 \tag{2.8}$$

For the fluctuations $\delta F(t)$ in intensity we likewise get:

$$\delta F(t) = q \cdot Q \cdot \int_V I_{em}(\vec{r}) \cdot \delta C(\vec{r},t) dr^3 \tag{2.9}$$

Substituting Eq.2.8 and Eq.2.9 into Eq.2.5, we get the following expression for the correlation function [2]:

$$G(\tau) = \frac{\int_V \int_{V'} I_{em}(\vec{r}) \cdot I_{em}(\vec{r}') \cdot \langle \delta C(\vec{r},t) \cdot \delta C(\vec{r}', t+\tau) \rangle dr^3 dr'^3}{(\int_V I_{em}(\vec{r}) \cdot \delta C(\vec{r},t) dr^3)^2} \tag{2.10}$$

Fick's second diffusion law, Eq.2.3 can be used to get an expression for the 'concentration correlation function' $\langle \delta C(\vec{r},t) \cdot \delta C(\vec{r}', t+\tau) \rangle$:

$$\langle \delta C(\vec{r},t) \cdot \delta C(\vec{r}', t+\tau) \rangle = \frac{\langle C \rangle}{(4\pi D_\tau \tau)^{\frac{3}{2}}} \cdot exp\left(-\frac{(\vec{r}-\vec{r}')^2}{4D_\tau \tau} \right) \tag{2.11}$$

The laser focus is assumed to have Gaussian cross-sections, both in the radial and the axial direction (Fig.2.4). This gives [2]:

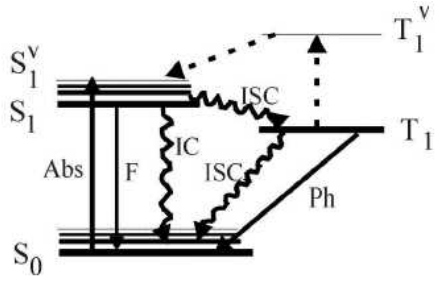

Figure 2.5: Energy diagram for the possible excitation and emission processes [2].

$$I_{em}(\vec{r}) = q \cdot Q \cdot I_0 \cdot exp\left(-2 \cdot \frac{x^2+y^2}{r_0^2}\right) \cdot exp\left(-\frac{2z^2}{z_0^2}\right) \tag{2.12}$$

where x and y are coordinates in the central plane of the focus, r_0 and z_0 are parameters that indicate the size of the focus (the radial and axial distances, respectively, from the center of the focus).

Substituting Eq.2.11 and Eq.2.12 into Eq.2.10, and solving numerically, we get the following expression for the correlation function:

$$G(\tau)_{3D} = \frac{1}{\langle N \rangle} \cdot \left(\frac{1}{1+\frac{\tau}{\tau_D}}\right) \cdot \left(\frac{1}{\sqrt{1+\frac{r_0^2\tau}{z_0^2\tau_D}}}\right) \tag{2.13}$$

The subscript $3D$ indicates, that this function corresponds to diffusion in three dimensions, and τ_D is the mean diffusion time, described by:

$$\tau_D = \frac{r_0^2}{4D_\tau} \tag{2.14}$$

As mentioned in the introduction, when we deal with lipid monolayers, we need only consider lateral diffusion, i.e. diffusion in 2 dimensions, when performing FCS on lipid monolayers. In this case, we can consider z_0 to be infinite, and Eq.2.13 gives:

$$G(\tau)_{2D} = \frac{1}{\langle N \rangle} \cdot \left(\frac{1}{1+\frac{\tau}{\tau_D}}\right) \tag{2.15}$$

As will be desribed in section 3.2, one has to perform FCS on a 3-dimensional sample of diluted Rhodamine, in order to calibrate the setup, before one can measure the desired quantities on the monolayers. Therefore, both equations 2.13 and 2.15 will be used.

2.4 Excitation and emission processes of fluorophores

Knowing the radiative processes taking place in an FCS experiment is essential for an understanding of it. Fig.2.5 shows the different possibilities for an excited dye molecule.

A dye molecule is excited from its ground state S_0 to a vibrational excited singlet state S_1^v by absorption of a laser photon ('Abs' in Fig.2.5). The molecule then decays to the non-vibrational excited level S_1. From here, the molecule can reach the ground state in one of the following ways; the most probable is the emission of a single photon ('F' in Fig.2.5). This is the *fluorescence*, we wish to measure. The other possibilities give rise to less efficient fluorescence emission. One of these is a radiationless internal conversion ('IC' in Fig.2.5), where the molecule decays from S_1 to a vibrational ground state S_0^v. Another is a radiationless intersystem crossing ('ISC' in Fig.2.5), in which the molecule enters a metastable triplet state T_1^v, lying below the S_1 state in energy, and then relaxes to the vibrational ground state S_0^v. This is called *phosphorescence*. There is also the possibility, that the molecule goes back to the excited S_1 state, to enter the same set of possibilities it started out with.

The phosphorescence is preferably avoided, because it gives rise to a deformation of the correlation curve. Therefore, one must try to counteract transitions to the metastable triplet state. One can do this by using a low laser power, and by introducing a quencher of the triplet state, for instance oxygen, into the system [18].

Chapter 3

Materials and methods

As mentioned in the introduction, the experimental procedure followed in this thesis is completely new. The entire setup is a combination of a Langmuir setup (section 3.1) and an FCS setup (section 3.2), to which a fluorescence microscope (section 3.3) is easily connected. This section describes each part of the entire setup.

3.1 Langmuir technique

The Langmuir setup contains a rectangular trough (Kibron MicroTrough X) with teflon barriers, two of which are movable (Fig.3.1), a small diameter $(0.51\ mm)$ special alloy wire connected to Kibrons proprietary microbalance, a temperature sensor and a Temperature Control Plate connected to a circulating water bath. The whole setup is connected to a computer with installed software from Kibron.

Before measurements, the trough, barriers, and alloy wire were cleaned carefully with ethanol and deionized water. Afterwards, they were dried with gaseous nitrogen. The wire was also held over a flame from a small lamp using ethanol as fuel. Contaminants are most unwelcome in Langmuir experiments, since a small dust particle would most likely reside on the water surface, when water is poured in the trough. With extra molecules on the surface, the surface pressure would rise faster on compression, than with lipids alone, thereby yielding error to the measurements.

After cleaning, deionized water was poured in the trough, and to test for possible contaminants, the water surface was compressed. Water can diffuse under the movable barriers, but since the water level is higher than the bottoms of the barriers, any contaminant surface molecules will remain between them. During compression, the water surface will experience a rise in pressure, if contaminated. A compression is done as follows:

The barriers are moved to the ends of the trough, and the surface pressure set to zero. Next, the barriers are set to move slowly together (about $140\ mm/min$. The small alloy wire is only just in contact with the water at its tip. Any possible rise in pressure is registered by the microbalance, in which the wire hangs, and during the whole compression, the surface pressure is monitored on the computer by means of the Kibron software, directly on the computer screen.

If the compression showed, that there were contaminants on the water surface (I accepted surface pressure rises of up to $0.1\ mN/m$), I sucked water from the sur-

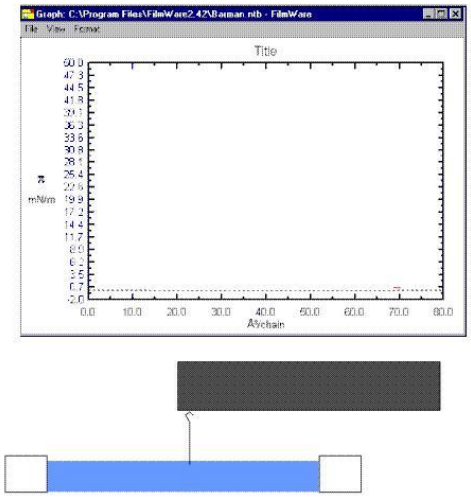

Figure 3.1: A schematic diagram of the trough with movable barriers and the alloy wire hanging in the microbalance. Also shown is the surface pressure/area diagram in which Kibron's software plots values while the experiment takes place (from http://www.kibron.com/).

face with a clean pipette tip connected to a vacuum, in the hope of also removing the unwanted contaminants. Then I poured in fresh water and repeated, until the water surface could be considered clean. At the end of this procedure, the setup was ready for experiments.

3.1.1 Creation of a lipid monolayer

The lipid monolayers were made by placing dissolved lipid molecules lightly on the water surface.

In order to do this, the DMPC lipids were first dissolved in a mixture of hexane and methanol, which are organic solvents. The isotherms presented later in this thesis were observed with a solution consisting of $1.4\ mg$ DMPC, $1.4329\ g$ hexane and $0.0416\ g$ methanol, which gives a total concentration of $0.630\ mg/ml$ for the lipids in solution, using the densities $0.66\ g/ml$ for hexane and $0.79\ g/ml$ for methanol. Before preparing the solution, the glass tube was rinsed thoroughly with deionized water, ethanol and hexane, and dried completely, so the concentration could be calculated correctly. When the solution was made, the glass tube with contents was immersed in an ultra sound water bath, in order to complete the dissolution of the lipids.

A proper amount of lipid solution was taken from the glass tube with a Hamilton syringe with a capacity of $10\ \mu l$. Beforehand, the syringe had been cleaned out with chloroform (a very effective organic solvent, that I have deliberately avoided when making the solution, for sanitary reasons). In the section 4.1 of this thesis, I have included two DMPC isotherms (made without using the FCS setup, i.e. without worrying about diffusion constants). One is made with $14.00\ \mu l$ ($13.09\ nmol$ lipids) of the solution, the other with $13.00\ \mu l$ ($12.15\ nmol$ lipids). The measured solution was slowly transferred from the syringe to the water surface, one small drop at a time,

with the tip of the syringe placed carefully on the surface. One must try to spread the molecules as much as possible by placing drops at different places of the surface, but stay relatively clear of the barriers of the trough, since the lipids might stick to these. After spreading the film, I waited a couple of minutes for the solvent molecules to evaporate. After this, I had a monolayer film of DMPC molecules at the air-water interface.

3.1.2 Measuring an isotherm

An isotherm is measured in the same manner as the water surface was tested for contaminants, that is, by compressing the water surface. With a lipid monolayer, though, one has to compress very slowly, to avoid random lipid structures. In both isotherms presented in this thesis, I have compressed with a speed of $5\ mm/min$. Again, the surface pressure can be followed directly on the computer screen, while compression takes place.

During measurement, the temperature in the trough is held constant at $20\,^{\circ}\mathrm{C}$ with the Temperature Control Plate, which is placed directly under the trough. The temperature is monitored by keeping the temperature sensor in contact with the water surface. The temperature registered by the sensor can also be monitored on the computer at all times.

The resulting isotherms are presented in section 4.1.

When measuring diffusion constants as a function of pressure, the Langmuir setup is used in combination with the FCS setup described in the following subsection.

3.2 Fluorescence Correlation Spectroscopy

The FCS setup, constructed by A. Hac and explained in detail in [2], is shown in Fig.3.2. The Nd:Yag laser emits a beam of green laser light of wavelength $532\ nm$, power $5\ mW$ and a diameter of $0.36\ mm$.

A telescope consisting of two quartz lenses with focal lengths $5\ mm$ and $100\ mm$ magnifies the beam 20-fold ($\frac{100\ mm}{5\ mm} = 20$) to $7.2\ mm$. In order for the foci of the lenses to coincide, they are placed $10.5\ cm$ apart.

The laser power of the beam is then regulated by passing it through a filter of proper optical density, or OD. The filter is placed between the telescope and the dichroic beam splitter in Fig.3.2. Optical density is defined as follows [2]:

$$OD = \log_{10} \frac{Power}{Power\ after\ OD\ filter}. \tag{3.1}$$

There are 6 possible filters to use in the setup (one of which is actually a position of no filtration with $OD = 0$). The 6 different OD's and the corresponding laser powers after filtration, are shown in the following table:

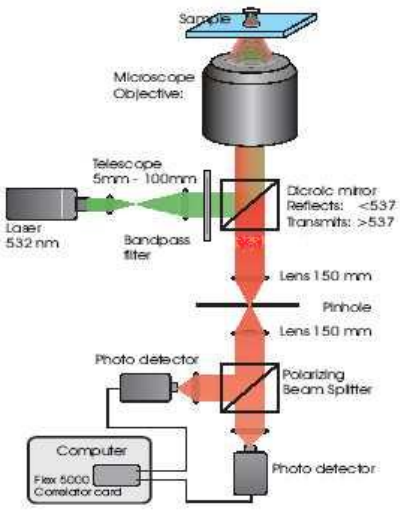

Figure 3.2: The FCS setup, slightly modified after [5].

OD filter	Laser power (mW)
0	5
0.1	3.97
0.6	1.26
1	0.5
2	0.05
3	0.005

The dichroic beam splitter reflects light of wavelengths shorter than $537\ nm$ and transmits light of wavelengths longer than $537\ nm$. The initial beam of wavelength $532\ nm$ is therefore reflected into the microscope objective (Fig.3.2).

The objective, which is an air objective with a working distance of $2.5\ mm$ and a focal length of $2500\ nm$, has a diameter of $7.2\ mm$, where the beam enters (the same as our beam), which is why the beam was magnified 20-fold in the first place. When the beam leaves the objective, it has been focused 40 times onto the sample which is placed right above it. When a fluorophore in the sample is hit by the laser light, it is excited to a higher energy state. It then immediately decays, emitting a photon with the corresponding energy difference. The emitted photon of a dye molecule used in experiments like these will have a wavelength larger than $537\ nm$. This means, that those photons that are released back into the objective, will be transmitted through the dichroic beam splitter.

From here they reach the so-called *pinhole*, which is another set of quartz lenses, both of which have focal lengths of $150\ mm$. The principle of the pinhole is to collect only fluorescence from near the central plane of the laser focus.

As Fig.3.3 shows, fluorescence emitted from the central plane of the focus hits the first pinhole lens perpendicularly, is focused on the pinhole and allowed to travel all the way to the detectors. Fluorescence emitted far away from the central plane, will hit the pinhole lens with an angle, that causes it to be scattered away from the pinhole.

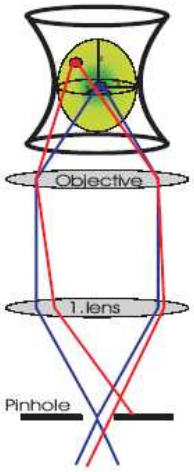

Figure 3.3: Diagram of the pinhole [5].

The polarizing beam splitter in Fig.3.2, divides the fluorescent light in parallel and perpendicularly polarized light. The beam splitter is part of the setup, but actually not relevant for the experiments performed for this thesis.

Finally, the light is focused onto the detectors by quartz lenses with $100\ mm$ focal lengths, and correlated on a computer connected to the setup through a Flex 5000 correlator card.

3.2.1 Calibrating the setup with Rhodamine

Before performing measurements on molecules with unknown diffusion constants, one must always calibrate the FCS setup, using fluorescent molecules with known diffusion constants, in order to measure the exact size of the radius of the laser focus. In this project, this was done with Rhodamine 6G (R6G) molecules in aqueous solution. R6G has the diffusion constant $D_\tau = 3 \cdot 10^{-6}\ cm^2/s$ at 296 K [2]. Thorough cleaning of every piece of material in direct contact with the samples is also an important part of the fluorescence experiments. The Rhodamine samples were prepared through careful cleaning of the containers and pipettes used, with ethanol and deionized water, and subsequent drying with nitrogen gas. The Rhodamine in solution had a concentration of $10\ nM$. Before measurements, a flow of oxygen was sent through the samples in order to quench the phosphorescence mentioned in section 2.4.

As mentioned earlier, the correlation function for the 3-dimensional diffusion of R6G is described by (Eq.2.13)

$$G(\tau)_{3D} = \frac{1}{\langle N \rangle} \cdot \left(\frac{1}{1 + \frac{\tau}{\tau_D}} \right) \cdot \left(\frac{1}{\sqrt{1 + \frac{r_0^2 \tau}{z_0^2 \tau_D}}} \right)$$

Since D_τ is known for R6G, the focus radius can be calculated through the relation

$$r_0^2 = 4 D_\tau \tau_D,$$

once the mean diffusion time, τ_D, has been read off a measured correlation curve of R6G.

This type of calibration is performed before every set of measurements, in case something has by accident changed a little bit in the setup, since the last time it was used (and in a crowded laboratory, something always has). The measured radius is then used to calculate diffusion constants in the sample of interest:

$$D_\tau = \frac{r_0^2}{4\tau_D}$$

The correlation curve depends on the filter used. Different correlation curves yield different τ_D's, which again yield different values for the radius. Before the FCS experiments on lipids, FCS on R6G was done with all 6 filters, in order to know the focus radius for the filter used for the lipid analysis, which was later decided on.

3.2.2 Labelling the lipids with fluorescent dye

For the FCS measurements presented in this thesis I used the same DMPC solution, that I prepared and used for making DMPC isotherms. The dye used is TRITC (Tetramethyl Rhodamine Iso-ThioCyanate).

The fluorophores are simply added to the readymade lipid solution and heated to approximately $50\,^\circ\mathrm{C}$, to make sure, that the dissolution is complete. The ultra sound water bath is avoided, because the vibration might make it difficult for the fluorophores to stick to the lipids.

I made several sets of measurements, some with 1 TRITC molecule per 10^6 lipids ($1\ ppm$), and some with $\frac{1}{2}\ ppm$, with similar results. FCS measurements were also performed completely without adding dye. The fact that these results were similar to the ones with added TRITC, indicates that the material used is not completely cleaned off, even after the standard procedure of washing with ethanol and deionized water. The graphs relating D_τ to MMA and pressure, respectively, presented in section 4.2.2 actually represent measurements without added dye. This experiment is similar to the ones with added dye, only far more vaues have been measured, and thereby more information obtained. This is the reason it has been chosen for presentation in this thesis.

3.2.3 FCS on DMPC monolayer

The Langmuir trough is placed right above the objective mentioned in the introduction to section 3.2. It is placed on a small table designed for the purpose. The table is kept horizontal at all times, and the distance between the table and the objective can be adjusted to the order of $0.1\mu m$.

The labeled lipid solution was spread in a monolayer at a clean water surface, as described in section 3.1.1.

After the laser was turned on, a few measurements were performed with different OD filters. The correlation takes place during the measurement, and can be followed on the computer. Since fluorophores are 'bleached' by the laser light (that is, a fluorophore can only absorb and emit a photon a limited number of times [5]), a low

laser power, equivalent to a high OD, is preferred. This also reduces the phosphorescence mentioned in section 2.4. The filter with the highest OD, that still yielded useful correlation curves, was chosen for the actual diffusion measurements. In the set of measurements presented in this thesis, the filter with $OD = 2$ has been used.

Any motion of the molecules, that does not originate from the random diffusion of the particles is (of course) undesired in an experiment measuring diffusion constants. Therefore, the actual compression of the monolayer took place, when not measuring, and the water bath and temperature control plate were only turned on, when not measuring, e.g. while compressing.

I measured correlation curves for different pressures. The fluorescence intensity was each time measured and correlated over a period of $300\ s$. Recall, that the correlation curves for monolayers are described by Eq.2.15:

$$G(\tau)_{2D} = \frac{1}{\langle N \rangle} \cdot \left(\frac{1}{1 + \frac{\tau}{\tau_D}} \right)$$

The correlation curves were analysed according to the method mentioned in section 3.2.1, in order to find the diffusion constants.

3.3 Fluorescence Microscopy

The same setup is used for Fluorescence Microscopy as for FCS, only with a few adjustments.

Three quartz lenses with focal lengths $30\ mm$, $100\ mm$ and $500\ mm$ (in that order) were put in between the telescope (Fig.3.2) and the filter (of $OD = 0$), in order for the laser beam to enter the objective focused, and exit the objective enlarged (in contrast to what was done, when performing FCS. Here, the beam entered the objective with a diameter of $7.2\ mm$, and was focused onto the sample by the objective). The illuminated region of the sample is in this manner about $150 \times 150\ \mu m$.

An Apogee Instruments Inc. camera was put right behind the dichroic mirror to record the emitted patterns of light from the sample. The detectors from the FSC experiments were not used.

A DMPC solution with concentration $1.9\ mg/ml$ was prepared with 1% TRITC added in proportion to lipids. A film of $5.2\ \mu l$ ($14.55\ nmol$ lipids) was spread on the water surface in the Langmuir trough, and the film compressed while microscopy images were recorded. The compression speed was $5\ mm/minute$ until a pressure of $10\ mN/m$ was reached, then the speed was lowered to $1\ mm/minute$. At about $25\ mN/m$, the speed was again lowered, this time to $\frac{1}{2}\ mm/minute$. The reason the speed was lowered along the way, was to capture the most interesting changes of the lipid structure.

The first set of images were recorded at $20\,^{\circ}\mathrm{C}$. Since there were no visible domains (section 2.1), the temperature was lowered to $16\,^{\circ}\mathrm{C}$. Again, no visible domains formed. The temperature was then lowered to $10\,^{\circ}\mathrm{C}$, the lowest temperature possible with the setup, and at this temperature, domains were finally visible.

The reason that domains become visible at all in a microscopy experiment is, that the TRITC molecules have a greater solubility in fluid phases than in gel phases. In

case of coexistence, the labels will 'prefer' to surround themselves with fluid lipids, and solid domains will appear as dark regions.

Chapter 4

Results

4.1 DMPC isotherms

The isotherms resulting from the procedure described in section 3.1 are shown in Fig.4.1.

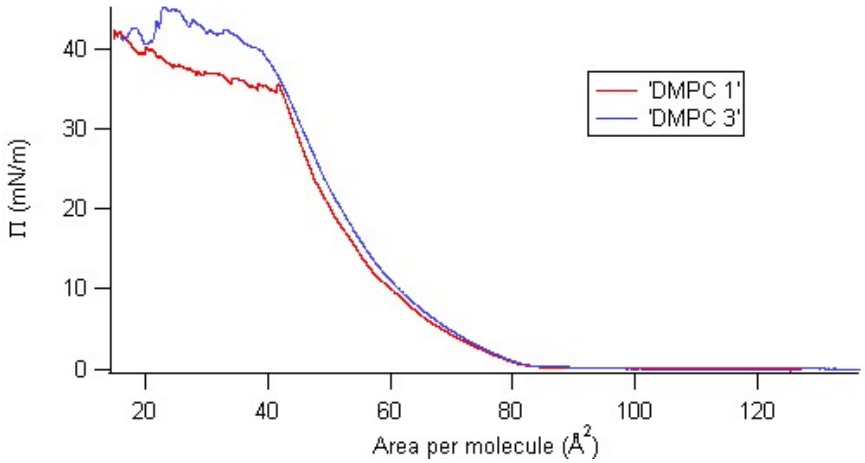

Figure 4.1: Measured DMPC isotherms.

Both compressions were started at a large molecular area of more than $125\ \mathring{A}^2$. At first we see no rise in the surface pressure π. At this baseline, the lipid molecules are not yet forced together, and the membrane is in the fluid state. As the membrane is compressed further, there is a point in which both isotherms start to show an increase in π, at about $85\ \mathring{A}^2$. This is the point, at which the molecules are all joined. From here, π rises slowly at first, and then faster. There is no visible plateau in these isotherms, hence the domains should be small at $20\,^{\circ}\mathrm{C}$. This was also tested with the aid of Fluorescence Microscopy. There were no visible domains. The reason for this is, that we are close to the melting temperature of DMPC, which is between $23\,^{\circ}\mathrm{C}$ and $24\,^{\circ}\mathrm{C}$. The Fluorescence Microscopy images, presented later in this chapter, clearly show domains at $10\,^{\circ}\mathrm{C}$, since this is far enough from the melting temperature for a significant amuont of the lipids to be in the solid ordered state. At about $40\ \mathring{A}^2$, the lipid structures of the monolayers collapse.

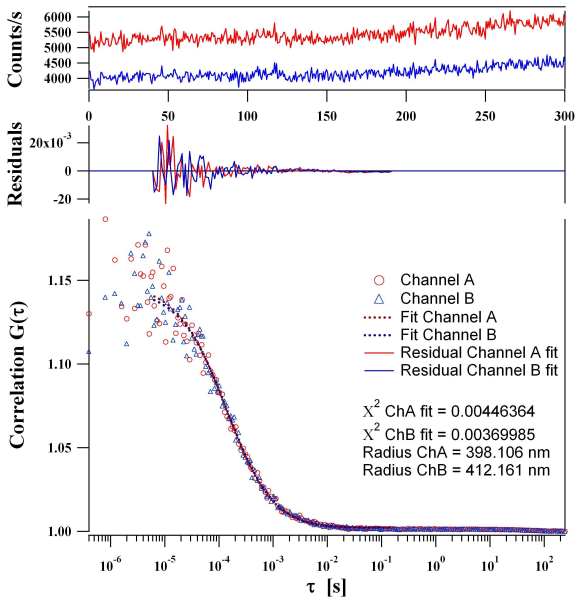

Figure 4.2: Measured Rhodamine intensity curve (top), the residual curves (middle) and correlation curve (bottom).

4.2 FCS results

4.2.1 Rhodamine measurements

The correlation curve for the FCS measurement on Rhodamine, that has been used to calculate the focus radius, is shown in Fig.4.2.

At the top, the fluorescence intensity measured by each of the two detectors is shown. The middle curve is the 'residual' curve, and it shows how much the correlation points deviate from the fitted correlation curve. A satisfactory residual curve has values rather symmetrically distributed around zero. If there is a pronounced tendency for the values to be either positive or negative, it means that the fit is not very good. At the bottom, the actual correlation curve is shown.

The filter used had $OD = 2$, and the temperature was kept constant at $20\,^{\circ}\mathrm{C}$ with the Temperature Control Plate and circulating water bath mentioned in section 3.1. The experimental software finds the τ_D used to calculate the radius in equation 3.2.1, and performs this calculation. The radius is taken as the average of the radius calculated for each detector. The radius is in this way found to be $405\ nm$. The mean diffusion time is then $\tau_D = 1.4 \cdot 10^{-4}\ s$, which seems reasonable, if one looks at the curve.

4.2.2 Diffusion constants of DMPC

After the focal radius had been determined, it was possible to measure diffusion constants of labeled DMPC lipids in monolayers. It was done following the method explained in section 3.2.3. One of the DMPC correlation curves is shown in Fig.4.3.

During the measurements, the temperature was again kept constant at $20\,^{\circ}\mathrm{C}$. The filter used was of course the same, as the one used for Rhodamine. For each of

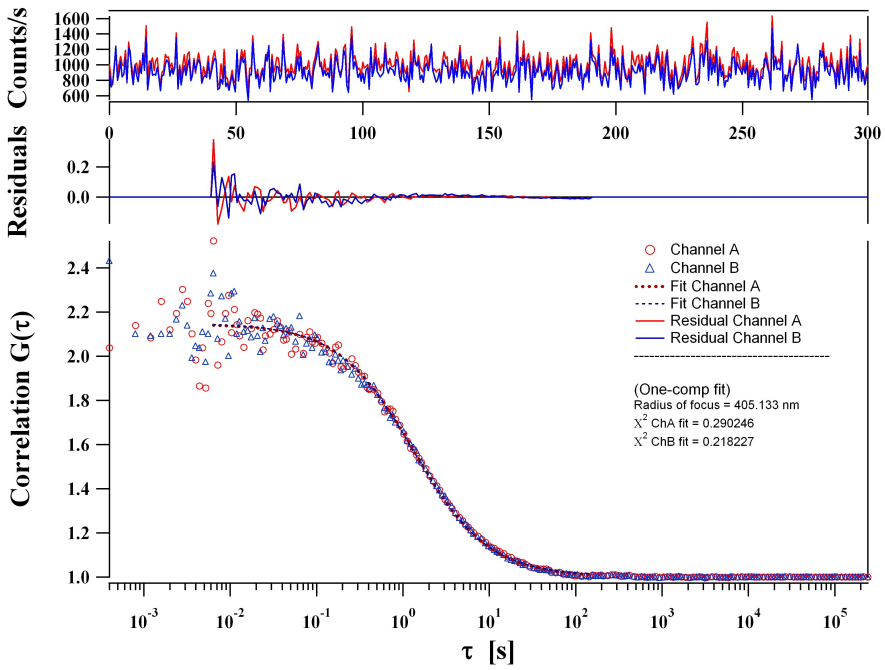

Figure 4.3: A correlation curve for the DMPC monolayer, recorded at a pressure of 11 mN/m and an MMA of 48 $\AA^2$.

the chosen pressure values, an FCS measurement was performed for 300 seconds. The compression was done with a speed of 0.34 $\AA^2/chain/minute$ corresponding to 0.77 $mm/minute$.

The measured diffusion constants are shown in Fig.4.4 and Fig.4.5.

There seems to be a clear tendency for the diffusion constant to increase with the MMA, and thereby to drop with increasing pressure.

Both graphs show that the diffusion constant of DMPC molecules in a monolayer consisting of only this type of lipid is between $1 \cdot 10^{-7}$ (pure gel) and $4 \cdot 10^{-7}$ (pure fluid) in the existence pressure range of the monolayer at 20 °C (The values at $MMA = 91$ $\AA^2$ corresponding to a pressure of 1 mN/m and $MMA = 84$ $\AA^2$ corresponding to a pressure of 2 mN/m are probably better omitted, judging from the tendency of the values in general).

Comparing these values to the ones found by Agnieszka Hac in [2], also with FCS, for DMPC in bilayers, which are $1.48 \cdot 10^{-9}$ cm^2/s for gel lipids, and $4.84 \cdot 10^{-8}$ cm^2/s for fluid lipids, it is seen, that the values found for monolayers in this thesis are generally higher. It is quite realistic, that lipids in monolayers move faster than lipids in bilayers. One can imagine, that a lipid in a bilayer faces greater resistance to its motion than a lipid in a monolayer, because of the lipid chains in the oppositely directed layer (compare Fig.1.5 to Fig.1.6).

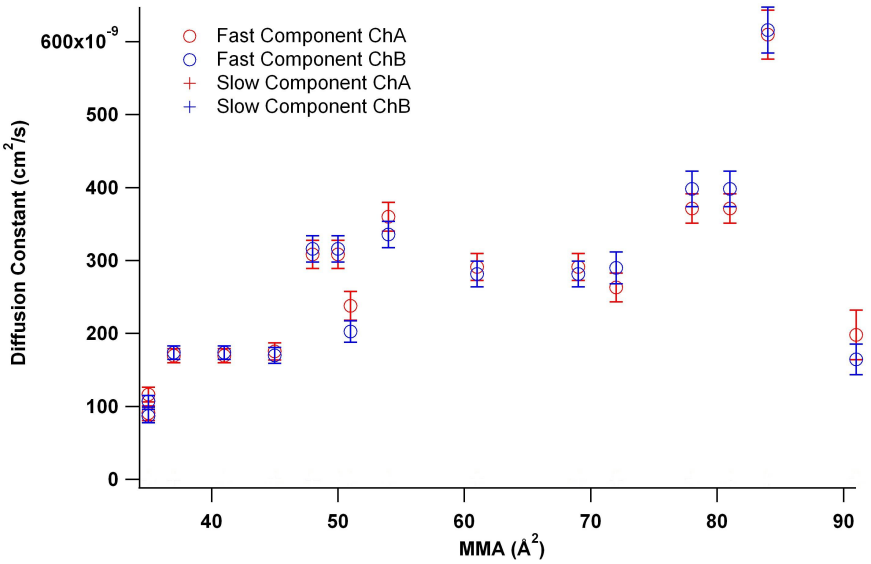

Figure 4.4: Diffusion constants of DMPC as a function of the mean molecular area.

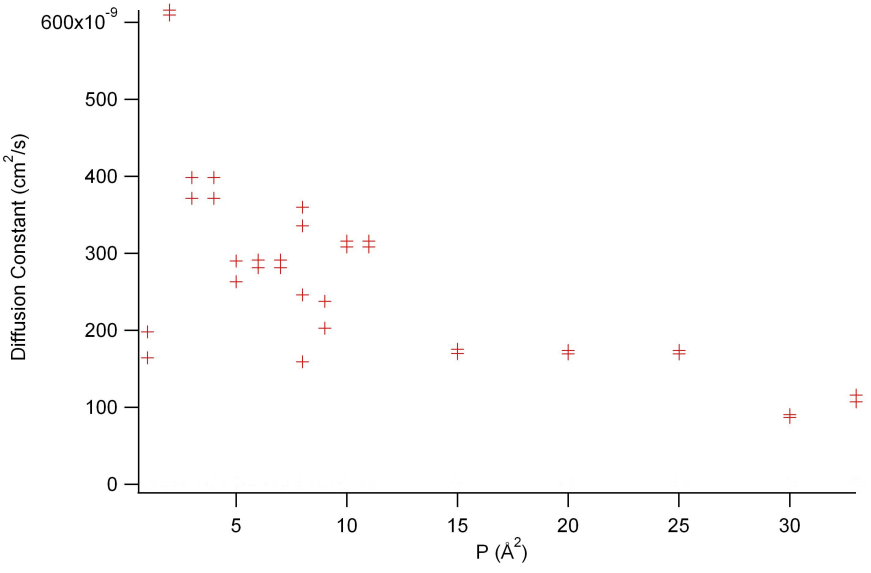

Figure 4.5: Diffusion constants of DMPC as a function of pressure.

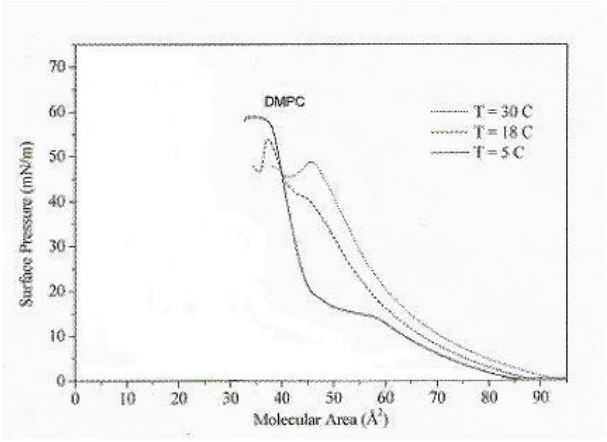

Figure 4.6: DMPC isotherms at 3 different temperatures. Slightly modified after [19].

4.3 Microscopy images of DMPC domains

Fig.4.6 shows three isotherms for DMPC, at different temperatures. In section 2.1 it was mentioned, that a visible plateau in an isotherm is an indication of visible domains, when performing microscopy. Therefore, from Fig.4.6, DMPC will show no such domains at $30\,^{\circ}\mathrm{C}$ and $18\,^{\circ}\mathrm{C}$, but there should be visible domains at around $5\,^{\circ}\mathrm{C}$.

Microscopy images were taken at $20\,^{\circ}\mathrm{C}$, $16\,^{\circ}\mathrm{C}$ and $10\,^{\circ}\mathrm{C}$. I have only included those at $10\,^{\circ}\mathrm{C}$ (Figs.4.7-4.11), since they are the only ones that show variation. The images at $20\,^{\circ}\mathrm{C}$ and $16\,^{\circ}\mathrm{C}$ look the same throughout the whole pressure range, because, as explained above, the domains are too small to be seen. $10\,^{\circ}\mathrm{C}$ is obviously a low enough temperature for visible domains to form in the $150 \times 150\ \mu m$ images.

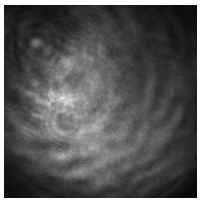

Figure 4.7: DMPC 1

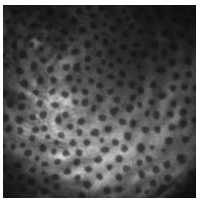

Figure 4.8: DMPC 2

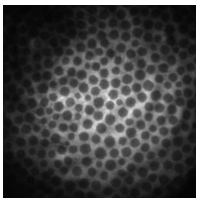

Figure 4.9: DMPC 3

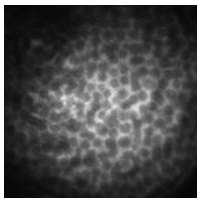

Figure 4.10: DMPC 4

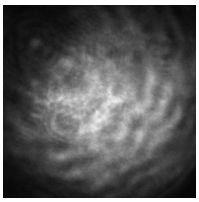

Figure 4.11: DMPC 5

At the two highest temperatures, where we have only fluid lipids, all the images appear continuously light (except for a pattern resulting from interference on the water

surface), in contrast to some of the images at $10\,^{\circ}\mathrm{C}$, where domains appear as dark spots. In this set of images, the images taken at very low (Fig.4.7) and very high pressure (Fig.4.11) also appear continuously light, since there is only one phase present. Small domains show up at a surface pressure of about $25\ mN/m$, and these increase in size and number, until they are no longer visible.

If one looks closely at the domain images, small spiral arms are visible around each domain. With this particular lipid (DMPC), the arms only appear as a blur. In other monolayers, for instance pure DPPC at $20\,^{\circ}\mathrm{C}$, the spirals are much clearer, and more beautiful. Figs.4.12-4.15 show such DPPC domains, recorded and kindly provided by Martin Gudmand from the Membrane Biophysics Group, NBI. They are recorded at a surface pressure of about $6\ mN/m$ with the same setup used for the DMPC images. The melting temperature of DPPC is about $41\,^{\circ}\mathrm{C}$, and because of this (and perhaps other factors), the domains are larger. Spiral arms form because of the symmetry of the molecules. A lipid is a chiral molecule, which means, that it cannot be superimposed on its own mirror image [10]. For more on lipid chirality, see [6], [7], [8] and [9].

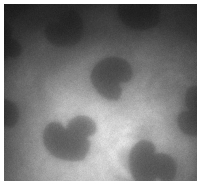

Figure 4.12: DPPC 1

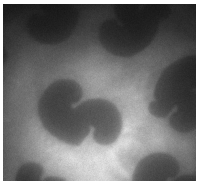

Figure 4.13: DPPC 2

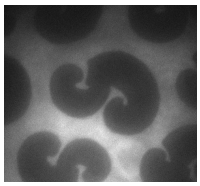

Figure 4.14: DPPC 3

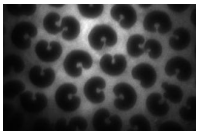

Figure 4.15: DPPC 4

4.4 Errors

There were uncertainties related to the preparation of the samples. The weighing of lipids and solvent is uncertain by $\pm 0.0001\ g$, causing uncertainties in the concentration of the samples. The Hamilton syringe used to spread the films is uncertain by $\pm 0.1\ \mu l$, which affects the certainty of the amount of lipid spread.

The cleaning procedure turned out not to be effective enough (section 3.2.2) to rinse off all dye from prior experiments. Since the same Langmuir trough has been used for all experiments for this thesis, they may all include effects of unintended molecules. The isotherms will, if there are more surface molecules than intended, appear to rise at a higher MMA than if there were the correct amount of surface molecules. Likewise, the MMAs stated in the FCS results could be larger, than they really are. Contaminant molecules of unknown kinds can also display unexpected ex-

citation and emission processes, so that the intensity pattern in the FCS experiments cannot be trusted competely.

Chapter 5

Conclusion

The aim of this thesis was to propose, how the diffusion constant D_τ of DMPC in a one-component monolayer varies with surface pressure (and MMA). This has been done, and with a quite realistic result.

D_τ is found to decrease with increasing pressure, which is what one would expect. Slower molecular motion is a natural consequence of increasing pressure on the system.

D_τ was also found to be a bit larger for DMPC in a monolayer than in a bilayer, by comparison with Agnieszka Hac's results [2] of FCS on DMPC bilayers. This is, as explained in section 4.2.2, also quite realistic.

Before the central FCS measurements, I measured isotherms of DMPC at $20\,^\circ\mathrm{C}$. By knowing how the surface pressure of the DMPC monolayer changed with temperature, and thereby the MMA- and pressure regions of interest (the region between the adjoining of the lipids and the collapse of the monolayer), I could make my FCS measurements at the most interesting pressures.

The isotherms and the FCS measurements were done at $20\,^\circ\mathrm{C}$ to make data treatment as simple as possible. It is more complicated to treat data resulting from systems containing different internal structures, like fluid and gel domains, with different diffusion constants. By performing the experiments at a temperature, for which the transition from the liquid to the solid state has a low cooperativity, the molecules change state independently of each other, and the average diffusion constant is easily obtained.

Finally, I have made Fluorescence Microscopy images of a DMPC monolayer to show the domain formation occurring in the region of coexistence between the gel and fluid phases. These were recorded both at temperatures of low and high cooperativity. The images at the lowest temperature (with the highest level of cooperativity) show visible domains. Lipid domains are sometimes seen with a clearer, spiral-shaped structure (e.g. the DPPC domains recorded by Martin Gudmand and shown in 4.3). The fact that the DMPC domains seen in the experiments for this thesis have a less clear structure is probably due to the fact, that they are also smaller. The reason they are smaller, probably has something to do with the low melting temperature for this particular lipid, as explained in section 4.3.

The performed FCS experiments on monolayers have been the first of their kind. The results obtained this way seem realistic, and there are definitely perspectives to

this approach.

Chapter 6

Acknowledgments

I would like to thank all the members of the Membrane Biophysics Group at NBI for all their help, and for being such good company. A special thanks to Martin Gudmand for his invaluable help and patience, and to Thomas Heimburg for support and good advice.

Bibliography

[1] T. Heimburg and M. Gudmand: Selvorganisering i biomembraner, article from KVANT, 2005, 3, pp. 22-24 (in danish)

[2] A. Hac: Diffusion Processes in Membranes Containing Coexisting Domains Investigated by Fluorescence Correlation Spectroscopy, Ph.D. thesis at the Physics Dept. Univ. Gttingen, 2003

[3] R. H. Tredgold: The physics of Langmuir-Blodgett films, review, Rep. Prog. Phys. 50, 1987, pp. 1609-1656

[4] V. M. Kaganer, H. Möhwald and P. Dutta: Structure and phase transitions in Langmuir monolayers, Reviews of Modern Physics, Vol. 71, No. 3, 1999, pp. 779-819

[5] A. Rosengren and P. B. Jensen: Investigating the motility of E.coli using Fluorescence Correlation Spectroscopy, Bachelor project in the Membrane Biophysics Group at the Niels Bohr Institute of Copenhagen, 2005

[6] H. M. McConnell: Structures and transitions in lipid monolayers at the air-water interface, Annu. Rev. Phys. Chem., 1991, 42, pp. 171-95

[7] C. W. McConlogue and T. K. Vanderlick: A Close Look at Domain Formation in DPPC Monolayers, Langmuir, 1997, 13, pp. 7158-64

[8] S. A. Kane, M. Compton, and N. Wilder: Interactions Determining the Growth of Chiral Domains in Phospholipid Monolayers: Experimental Results and Comparison with Theory, Langmuir, 2000, 16, pp. 8447-55

[9] P. Krüger and M. Lösche: Molecular chirality and domain shapes in lipid monolayers on aqueous surfaces, Physical Review E, 2000, Vol. 62, nr. 5, pp. 7031-43

[10] P. Atkins and J. de Paula: Atkins' Physical Chemistry, 7th ed., Oxford University Press, 2002

[11] Nobel Lectures, Chemistry 1922-1941, Elsevier Publishing Company, Amsterdam, 1966

[12] M. Lösche and H. Möhwald: Fluorescence microscope to observe dynamical processes in momomolecular layers at the air/water interface, Rev. Sci. Instrum. 55(12), 1984, pp. 1968-72

[13] D. Magde, E. L. Elson and W. W. Webb: Fluorescence Correlation Spectroscopy. An Experimental Realization, Biopolymers, Vol. 13, 1974, pp. 29-61

[14] G. Palumbo and R. Pratesi: Lasers and Current Optical Techniques in Biology, European Society for Photobiology, 2004

[15] P. B. Moore, C. F. Lopez, and M. L. Klein: Dynamical Properties of a Hydrated Lipid Bilayer from a Multinanosecond Molecular Dynamics Simulation, Biophysical Journal, Vol. 81, 2001, pp. 24842494

[16] Robert. A. Alberty and Robert. J. Silbey: Physical Chemistry, Second Edition, John Wiley & Sons, Inc., 1996

[17] W. W. Webb: Fluorescence Correlation Spectroscopy: Genesis, Evolution, Maturation and Prognosis, Fluorescence Correlation Spectroscopy; Theory and Applications, Springer Verlag, 2000, pp. 307-330

[18] J. Widengren, Ü. Mets and R. Rigler: Fluorescence Correlation Spectroscopy of Triplet States in Solution: A Theoretical and Experimental Study, J. Phys. Chem. 1995, 99, pp. 13368-13379

[19] F. Gaboriand, R. Volinsky, A. Berman, R. Jelinek: Temperature dependence of the organization and molecular interactions witin phospholipid/diacetylene Langmuir films, Journal of Colloid and Interface Science, Vol. 287, Issue 1, 2005, pp. 191-97

[20] H. Seeger, M. Fidorra, and T. Heimburg. 2005. Domain size and fluctuations at domain interfaces in lipid mixtures, Macromolecular Symposia (Wiley) 219, pp. 85-96

[21] V. Oliynyk: Experimental study of lipid membranes: lipid domain formation and peptide aggregation, Ph.D. thesis at Membrane Biopysics Group at the Niels Bohr Institute of Copenhagen and the Physics Dept. Univ. Gttingen, 2005

[22] T. Heimburg: Fluctuations and domains: Thermodynamic properties and heterogeneity of membrane assemblies, Max-Planck-Institut fr biophys.Chemie News (7/1998)

[23] M. R. Lance, C. Washington and S. S. Davis: Evidence for the Formation of Amphotericin B-phospholipid Complexes in Langmuir Monolayers, Pharmaceutical Research, Vol. 13, 7, 1996, pp. 1008-14